diversity

MDPI

Article

Systematics of the Arboreal Neotropical '*thorellii*' Clade of *Centruroides* Bark Scorpions (Buthidae) and the Efficacy of Mini-Barcodes for Museum Specimens

Aaron M. Goodman [1,2,*], Lorenzo Prendini [2] and Lauren A. Esposito [1]

[1] Institute for Biodiversity Science and Sustainability, California Academy of Sciences, 55 Music Concourse Drive, San Francisco, CA 94118, USA; lesposito@calacademy.org
[2] Division of Invertebrate Zoology, American Museum of Natural History, Central Park West at 79th St., New York, NY 10024, USA; lorenzo@amnh.org
* Correspondence: agoodman@amnh.org; Tel.: +1-415-672-0493

Abstract: Fragmented and degraded DNA is pervasive among museum specimens, hindering molecular phylogenetics and species identification. Mini-barcodes, 200–300-base-pair (bp) fragments of barcoding genes, have proven effective for species-level identification of specimens from which complete barcodes cannot be obtained in many groups, but have yet to be tested in arachnids. The present study investigated the efficacy of mini-barcodes combined with longer sequences of the Cytochrome *c* Oxidase Subunit I (COI) gene in the systematics of the arboreal Neotropical '*thorellii*' clade of *Centruroides* Marx, 1890 bark scorpions (Buthidae, C.L. Koch 1837), the species of which have proven to be difficult to identify and delimit due to their similar morphology. The phylogeny of 53 terminals, representing all nine species of the clade and representative species belonging to related clades of *Centruroides*, rooted on *Heteroctenus junceus* (Herbst, 1800) and based on up to 1078 base pairs of COI and 112 morphological characters, is presented to test the monophyly of the clade and the limits of its component species. The results support the recognition of nine species of the '*thorellii*' clade, in accordance with a recent taxonomic revision, and highlight the efficacy of mini-barcodes for identifying morphologically similar cryptic species using specimens of variable age and preservation.

Keywords: scorpions; taxonomy; phylogenetics; species delimitation; COI; genetic degradation; morphology

Citation: Goodman, A.M.; Prendini, L.; Esposito, L.A. Systematics of the Arboreal Neotropical '*thorellii*' Clade of *Centruroides* Bark Scorpions (Buthidae) and the Efficacy of Mini-Barcodes for Museum Specimens. *Diversity* **2021**, *13*, 441. https://doi.org/10.3390/d13090441

Academic Editor: Luc Legal

Received: 8 July 2021
Accepted: 10 August 2021
Published: 16 September 2021

1. Introduction

Although natural history collections constitute one of the largest repositories of genetic information and are paramount for biological research, successful amplification of DNA from museum specimens often proves difficult due to degradation and fragmentation [1,2]. Many museum specimens were not collected with the intention (or knowledge) of future genomic studies, resulting in varying methods of preservation both among and within taxa and varying rates of subsequent molecular degradation among specimens of similar age [2]. Several factors, including time, dehydration, environmental exposure, and the presence of bacterial or fungal contamination, markedly affect the quality of DNA in collections of vertebrate and invertebrate taxa [2–4]. Although DNA barcoding is cost-effective for species identification, the utility of this method for museum material is severely limited by the failure to amplify complete Cytochrome *c* Oxidase Subunit I (COI) sequences and the cost in finances, time, and effort to repeat amplifications for adequate coverage. Overcoming the obstacle of sequencing museum specimens is critical, as natural history collections provide the basis for studies of historical populations, the discovery of new (and often cryptic) species, and the verification of barcoded specimens to types [5–8].

Research suggests that barcodes as short as 200 nucleotide base pairs (bp), the length at which DNA from degraded museum material stabilizes [2,8], are sufficient

to acquire 95% confidence in species-level identification, thus promoting the use of 'mini-barcodes', primer sets designed to amplify 200–300-base-pair (bp) fragments of barcoding genes [8]. Mini-barcodes have proven effective for species-level identification from degraded museum specimens in a variety of systematics studies concerning fish, reptiles, mammals, insects, and plants, as well as for the identification of processed or traditional food products [8–15].

The Neotropical '*thorellii*' clade of *Centruroides* Marx, 1890 bark scorpions (Buthidae C.L. Koch 1837)—mostly inhabiting the forest canopy and characterized by their relatively small size, mottled coloration, and elongated metasoma and telson, more pronounced in the adult males—represents an ideal system for testing the efficacy of mini-barcodes in arachnids (Figure 1). Historically, *Centruroides hoffmanni* Armas, 1996, *Centruroides rileyi* Sissom, 1995, and *Centruroides schmidti* Sissom, 1995 were assigned together with *Centruroides thorellii* Kraeplin 1891 to the informal '*thorellii*' species group based on their similar morphology, habitat, and distribution in the forests of southern Mexico and northern Central America [16–20]. However, it was recently demonstrated that the '*thorellii*' species group is a paraphyletic assemblage, with *C. thorellii* being more closely related to a clade of dark, large-bodied species of *Centruroides*, suggesting that the apparent morphological similarity to other species of the '*thorellii*' group is convergent [21,22].

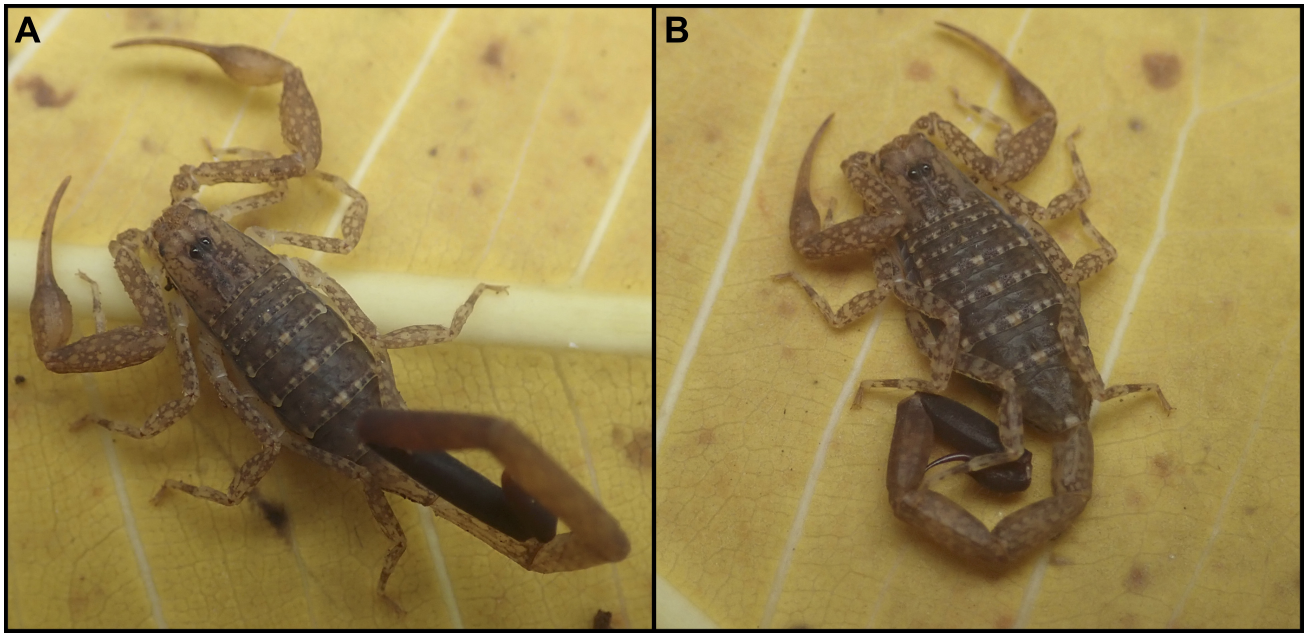

Figure 1. *Centruroides berstoni* (Goodman et al., 2021), a representative species of the arboreal Neotropical '*thorellii*' clade of *Centruroides* Marx, 1890 bark scorpions (Buthidae C.L. Koch, 1837), habitus in life: ♂ (**A**) and ♀ (**B**), Biotopo Chocón Machacas, Município Livingston, Guatemala.

The difficulty of collecting these canopy-dwelling scorpions appears to have resulted in their diversity and distribution being severely undersampled. Many collection records are represented by singletons. The comparative rarity of these scorpions in collections resulted in a tripling of the known diversity to a total of nine species in a recent revision [23], wherein six new species, previously identified as operational taxonomic units (OTUs) on the basis of DNA sequence data [22], were described. However, insufficient material prevented a decision as to whether the OTUs identified were new species or variable populations of more widespread species [22]. A larger sample of specimens from across the distribution permitted a more thorough assessment of species limits within the clade, resulting in the descriptions of *Centruroides berstoni* Goodman et al., 2021, *Centruroides catemacoensis* Goodman et al., 2021, *Centruroides chanae* Goodman et al., 2021,

Centruroides cuauhmapan Goodman et al., 2021, *Centruroides hamadryas* Goodman et al., 2021, and *Centruroides yucatanensis* Goodman et al., 2021.

The present study aimed to test the species limits and phylogenetic relationships among the species of the '*thorellii*' clade recognized by Goodman et al. (2021) using COI mini-barcodes of individuals from disparate localities combined with longer COI sequences and morphological characters, and in so doing demonstrating the efficacy of mini-barcodes for species-level identification of old and/or poorly preserved arachnid specimens from natural history collections [23].

2. Materials and Methods

Taxon Sampling

The ingroup comprised nine terminals, representing all nine species of the '*thorellii*' clade [23]. Each species was represented by three to seven individuals from one to five localities, including the type localities of all species except *C. hoffmanni*, *C. rileyi*, and *C. schmidti*, the identifications of which were verified based on morphology [16,19]. Exemplar species representing the North American, Central American, and Caribbean clades of *Centruroides* [21] were included as outgroups. Three species per clade were included to represent the genetic variability within each. Specimens of *C. thorellii* were also included to test its phylogenetic position. Trees were rooted on *Heteroctenus junceus* (Herbst, 1800), representing *Heteroctenus* Herbst, 1800, the sister taxon of *Centruroides* [21]. The complete taxon sample comprised nine ingroup species and ten outgroup species, considered satisfactory for testing the monophyly of the '*thorellii*' clade.

Material Examined

Specimens and tissue samples used for molecular and morphological analyses were obtained from the American Museum of Natural History (AMNH), New York; the California Academy of Sciences (CAS), San Francisco; the Colección Nacional de Arácnidos, Instituto de Biología (CNAN), Universidad Nacional Autónoma de México, Mexico City; and the Oxford University Museum of Natural History (OUMNH), UK.

Field-collected specimens from localities in Veracruz, Mexico, and southern Guatemala were detected using ultraviolet light, euthanized by submersion in 95% ethanol, and subsequently injected with ethanol to improve internal preservation. A total of 53 tissue samples, stored at −20 °C at the CAS and the Ambrose Monell Cryo Collection at the AMNH, were used for DNA extraction (Appendix A).

DNA Sequencing

Genomic DNA was extracted from muscle tissue from the fourth leg of well-preserved specimens using the spin column extraction protocol of the Qiagen DNeasy Blood & Tissue Kit (Valencia, CA, USA). DNA extracts were stored in 50–200 µL of elution (AE) buffer depending on the DNA concentration assessed using a Nanodrop 2000C Spectrophotometer (ThermoFisher Scientific, Waltham, MA, USA).

PCR amplification of complete mitochondrial and nuclear genes proved impossible for many older samples due to degradation and fragmentation of the DNA. Therefore, a 125-bp hypervariable region of the COI gene was partially amplified using the mini-barcode forward primer Uni-MinibarF1, 5′-TCCACTAATCACAARGATATTGGTAC-3′, and the reverse primer Uni-MinibarR1, 5′-GAAAATCATAATGAAGGCATGAGC-3′ [8]. Partial COI sequences, ca. 650 bp in length, were successfully amplified for field-collected specimens using the primers LCO1490 (5′-GGTCAACAAATCATAAAGATATTGG-3′) and HCO2198 (5′-TAAACTTCAGGGAGACCAAAAAATCA-3′) [24]. Complete COI sequences (1078 bp) were incorporated into the dataset from Esposito (2011) using the primers HCOEXTERNA (5′-GAAGTTTATATTTTAATTTTACCTGG-3′) and HCOEXTERNB (5′-CCTATTGAWARAACATARTGAAAATG-3′) [25].

Each PCR reaction was conducted in a 25-microliter volume, comprising 2.5 µL of 10× PCR buffer, 0.5 µL of dNTPs (10 mM stock), 1.0 µL of $MgCl_2$ (50 mM stock), 1.0 µL of each primer (25 mM stock), 1.0 µL of bovine serum albumin, 0.25 µL of Invitrogen

(Waltham, MA, USA) Taq polymerase enzyme (5 units/μL stock), 7.75 μL of Millipore (Burlington, MA, USA) deionized H_2O, and 10 μL of DNA template. Reactions with the LCO1490/HCO2198 primers used 2 μL of DNA template with 15.75 μL of Millipore deionized H_2O. PCR amplifications, performed on a BioRad MyCycler thermocycler (Bio-Rad Laboratories, Hercules, CA, USA) at the CAS Center for Comparative Genomics (CCG) and an Epicenter thermocycler (Eppendorf, Hamburg, Germany) at the AMNH Sackler Institute for Comparative Genomics (SICG), included an initial denaturing step at 95 °C for 2 min; 40 cycles of denaturing at 95 °C for 30 s, annealing at 47 °C for 30 s, and extension at 72 °C for 60 s; and a final extension at 72 °C for 10 min. PCR products were checked using gel electrophoresis on 1% agarose gel with ethidium bromide, and 1–2 μL of ExoSAP-IT (USB Scientific, Cleveland, OH, USA) was used to clean PCR products.

Sanger dideoxy sequencing was conducted using fluorescent-labeled BigDye Terminator 3.1 (Applied Biosystems, Waltham, MA, USA). Each 10-microliter reaction included 5.45 μL of Millipore deionized H_2O, 1.5 μL of 5× BigDye buffer, 0.3 μL of primer (10 mM stock), 0.75 μL of BigDye, and 2 μL of cleaned PCR product. The STeP50 Program (Platt et al., 2007) was used for cycle sequencing on a BioRad MyCycler thermocycler at the CAS CCG and an Epicenter thermocycler (Eppendorf, Hamburg, Germany) at the AMNH SICG. The labeled single-stranded DNA was precipitated by adding 2.5 μL of 125 mM di-NaEDTA to each sample, followed immediately by washing and centrifuging in 100% and 70% ethanol. Samples were then dried in a 65 °C incubator for 8 min, and 10 μL of HiDi formamide (Applied BioSystems) was added to each pellet, denatured at 94 °C for 2 min, and cooled on ice for 5 min. The denatured and fluorescent-labeled DNA pellets were sequenced on an ABI 3130x Genetic Analyzer (Applied BioSystems) at the CAS CCG and a Prism™ 3730x (Applied BioSystems) at the AMNH SICG.

Newly generated sequences were edited, forward and reverse primers were removed, and complementary strands were assembled into consensus sequences using Geneious v. 11.0.4 [26], by reference to a 1078-bp fragment of COI for *C. rileyi* from GenBank [21]. The dataset comprised 53 sequences, 14 mini-barcodes (127–134 bp), 12 partial (430–659 bp) sequences, 14 previously unpublished complete (1078 bp) sequences [21], and 13 complete sequences from Esposito and Prendini (2019) (Appendices 2 and 3) [22]. Sequences less than 150 bp in length were uploaded to the Dryad digital repository (doi:10.5061/dryad.fttdz08t2), whereas sequences greater than 150 bp in length were submitted to GenBank (Appendix B).

Morphological Character Matrix

Adult specimens from which DNA sequences were generated were scored using relevant characters from Esposito (2011), Esposito et al. (2017), and other sources (Table 1) [22,27]. The data matrix comprised 112 characters, including 43 (35%) from the prosoma, 38 (33%) from the mesosoma, and 30 (29%) from the metasoma, 41% derived from carination and surface macrosculpture, 25% from shape and morphometrics, 24% from coloration, and 7% from other character systems, e.g., macrosetae, trichobothria, and internal anatomy (Appendix C). Morphological examination of specimens was conducted using a Leica M125 stereomicroscope with an ocular micrometer calibrated at 10× magnification, with an LED-6WD UV spotlight to enhance the visualization of granulation and carination of the exoskeleton under ultraviolet light. Character states were scored from 0 to 5, as unknown (?) for missing data, or as polymorphic if two or more states were exhibited. The morphological terminology follows Hjelle (1990) and Sissom (1990), except for carapace and metasomal carination, which follows Vachon (1952); trichobothria, which follows Vachon (1974); tergite and pedipalp carination, which follows Prendini (2000); book lung anatomy, which follows Kamenz and Prendini (2008); and ovariuterine anatomy, which follows Volschenk et al. (2008) [28–34]. The matrix is deposited in Morphobank (http://morphobank.org/permalink/?P4047; accessed on 28 June 2021).

Phylogenetic Analysis

Sequences were aligned using the ClustalW method [35,36] in Mesquite v. 3.51 [37] and checked by eye. The average nucleotide composition of the aligned COI sequences was 17.7% A, 13% C, 25.2% G, and 44% T, and 725 sites were identical (67.4%), with 40.7% missing data as sequences varied greatly in length (125–1078 bp). Gaps in the dataset were treated as missing data and codon positions were optimized to reduce stop codons.

Phylogenetic relationships were inferred with a combined analysis of the molecular and morphological datasets using Bayesian inference (BI) in MrBayes v. 4.3.6 [38] and only the molecular dataset using maximum likelihood (ML) in RAxML v. 8.0.0 [39] on the CIPRES supercomputing cluster [40]. PartitionFinder2 [41] was used to determine the evolutionary models for BI and the partition definitions for ML. PartitionFinder2 obtained the highest AIC and BIC scores for the HKY+G model (for codons 1, 2, and 3); hence, that model was used for all subsequent analyses. Morphological characters were incorporated into the ML analysis and optimized using the gamma model of rate of heterogeneity and corrected for ascertainment bias using a Lewis correction type [42].

Table 1. Distribution of 112 morphological characters scored for phylogenetic analysis of the arboreal Neotropical '*thorellii*' clade of *Centruroides* Marx, 1890 bark scorpions (Buthidae C.L. Koch 1837) and outgroup species of *Centruroides* and *Heteroctenus junceus* (Herbst, 1800). Character states are scored from 0 to 5, as unknown (?), or as polymorphic [].

Outgroup
Heteroctenus junceus
2101131122 1120211321 0100011011 1212101013 0001112120 2000121000
0111020011 01120021?? 0101021011 1011001001 1111211110 11
Centruroides arctimanus
1010010011 0120221221 0000010?1? 111111210? 00111???20 2121000010
0110102?10 0111000??? ???1100000 1210000100 0110011110 00
Centruroides bani
0110021222 1120011121 0001010001 1011112000 0110011222 2112110000
0110101010 01110031?? ???1101001 1[01]10000 0011001111 11201
Centruroides exilicauda
0100030202 1120200010 0000010111 0000200000 0010113110 2110220011
0000201010 11110130?? 0111021111 1011101010 1101211110 11
Centruroides gracilis
1000011112 1120201321 0100111111 1212202000 0110003120 2120220011
0110201020 1102100100 0111001111 101?001011 1110011012 11
Centruroides hentzi
2010030122 0120200020 0000014110 1010102000 0101101112 2111010010
0111202020 00110000?? ???1101011 1210000000 1101211000 01
Centruroides infamatus
1000031212 1120200011 0000010111 1010102000 0010111111 2110121010
0110100010 01010020?? ???1001111 1210101011 1101011?12 11
Centruroides ochraceus
0000031202 1100211111 0100010?1 0000102000 00102???22 2110221011
0110101?21 01010100?? ???1101111 1010011011 1101211110 11
Centruroides thorellii
0000021101 1120200000 0100010110 0101102000 0010112301 2100120011
0110201020 01011001?? ???1100011 1301100010 0110000002 01
Centruroides tuxtla
0100131222 1120100021 0000010111 1011102005 0110202322 2111120011
0101102010 1112010??? ???1000011 1210100110 0010000012 01

Table 1. *Cont.*

Ingroup
Centruroides berstoni
1110010111 1000000010 0001010101?0 1010012115 0110002111 2112220011
0?00202?10 011101100?? ???1100000 0110000000 0111010101?0 01
Centruroides catemacoensis
1110010222 1021200010 0001010110 1010010115 0010202111 2110020010
0110202120 001001100?? ???1100000 0110000000 0111210000 01
Centruroides chanae
1110010111 1021200000 0001314110 1111010005 00112???12 2102220011
0?10202120 0111010??? ???1110000 0010000000 0111211010 01
Centruroides cuauhmapan
1110010110 1120200010 0000314110 1010012010 0111202121 2103120011
0?10202010 011101100?? ???1100000 0010000000 0111010000 01
Centruroides hamadryas
1110010111 1000000010 0001010101?0 1010012115 0110002111 2112220011
0?00202?10 011101100?? ???1100000 0110000000 0111010101?0 01
Centruroides hoffmanni
0100010111 1121000010 0000010110 1111012005 1110112110 2103220011
0?00202020 011101100?? ???1100000 0210000010 0110211010 01
Centruroides rileyi
1110010110 1120200010 0000314110 1010012010 0111202121 2103120011
0?10202010 011101100?? ???1100000 0010000000 0111010000 01
Centruroides schmidti
1110010111 0120200010 0101010110 1010012010 0100012122 2102220011
0000202120 111101010?? 0111100000 0010000000 0101211010 00
Centruroides yucatanensis
1110010111 1120000010 0001014110 1010012105 0010012021 2103020011
0?10201120 0111010??? ???1100000 0010000000 0110010112 01

A rapid bootstrap analysis was run with 1000 iterations. MrBayes was run twice on four threads for 50,000,000 generations, with Markov chains sampled every 1000 generations and the standard 25% burn-in calculated. Branches with posterior probability values $\geq$0.95 were considered strongly supported [43]. A 50% majority-rule consensus tree was created, and nonparametric bootstraps were estimated for the optimal nucleotide substitution model. Nodes with bootstrap values $\geq$70 were considered strongly supported [43].

Species Delimitation

The limits of putative species were evaluated on the majority-rule consensus tree from the Bayesian 95% posterior probability of the concatenated dataset of morphological characters and aligned DNA sequences using the species delimitation plugin in Geneious [26,44]. Clusters of sequences were evaluated based on their association with individuals collected at the type locality. Specimens which were monophyletic with those collected at the type locality or within the vicinity thereof with greater than 0.95 posterior probability were assigned to the species in question. Several metrics were investigated for assessing species delimitation in Geneious, including P (AB) for reciprocal monophyly [45]; P (RD), which measures the probability of an observed clade's degree of distinctiveness [46] and values for the probability of population identification of a hypothetical sample based on the groups being tested; P ID (Strict), and P ID (Liberal).

3. Results

Phylogenetic analyses with BI and ML produced almost identical tree topologies with well-supported terminal nodes but weakly supported internal nodes (Figures 2 and 3). Nine well-supported reciprocally monophyletic species-level clades were recovered in both analyses, but relationships within each clade received low support (Figures 2 and 3). *Centruroides hoffmanni*, *C. rileyi*, and *C. schmidti* received high posterior probabilities and

likelihood values for monophyly (0.99/100, 0.95/100, and 0.99/100, respectively). *Centruroides thorellii* was placed outside the '*thorellii*' clade (Figures 2 and 3). All recently described species were well-supported: *C. berstoni* (0.99/99); *C. catemacoensis* (1.00/100); *C. chanae* (1.00/100); *C. cuauhmapan* (0.99/100); *C. hamadryas* (0.98/82); *C. yucatanensis* (1.00/100) (Figures 2 and 3). The species delimitation analysis identified nine distinct species, all of which received values for Rosenberg's P (AB) lower than 0.01, supporting the results of the BI and ML analyses (Table 2).

4. Discussion

Systematics

The present study is the first analysis of scorpions in which COI mini-barcodes from museum specimens were used for species identification. Three nominal species and six OTUs, identified by Esposito (2011) and described as new species of the '*thorellii*' clade by Goodman et al. (2021), were confirmed by the analyses presented here, highlighting the efficacy of mini-barcodes for identifying morphologically similar cryptic species using specimens of variable age and preservation [22,23].

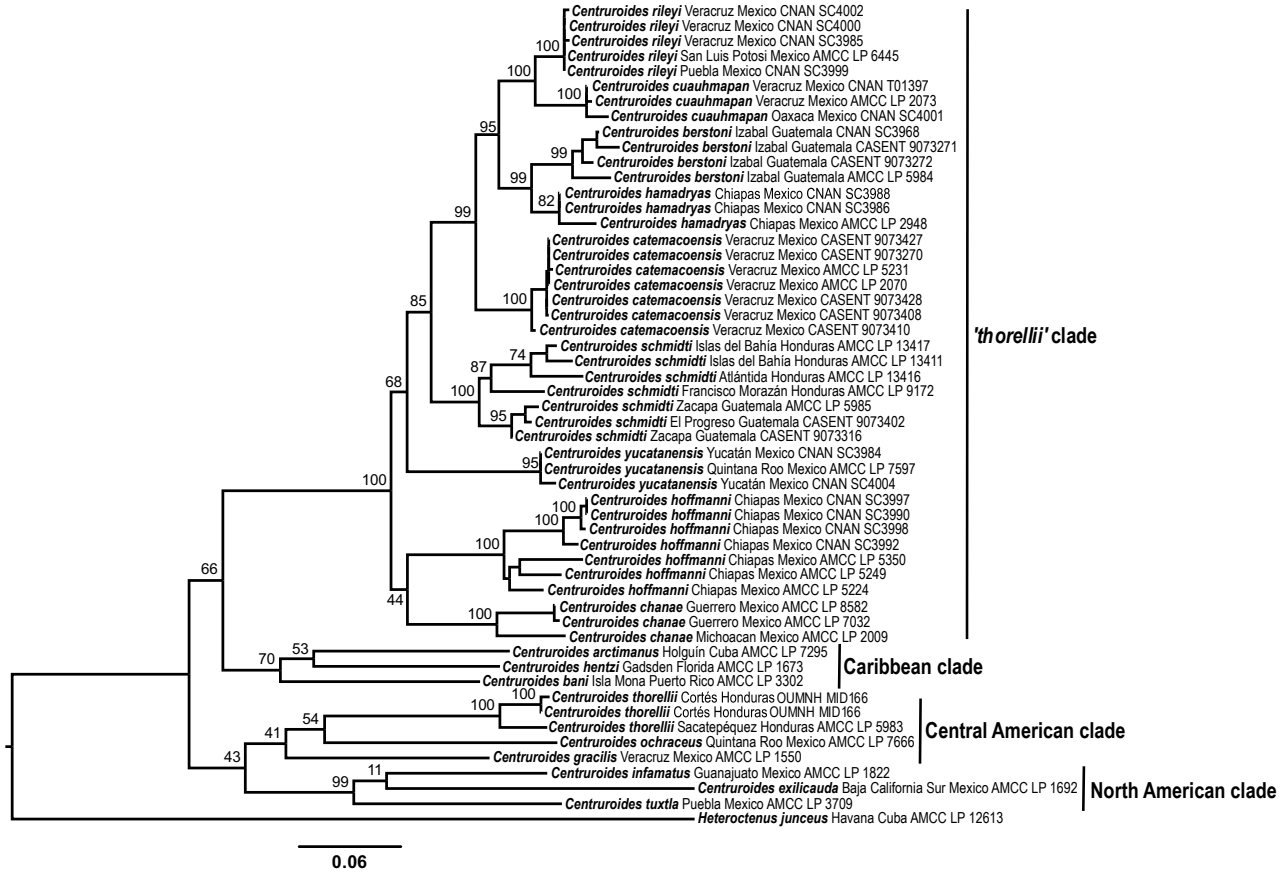

Figure 2. Phylogeny of the arboreal Neotropical '*thorellii*' clade of *Centruroides* Marx, 1890 bark scorpions (Buthidae C.L. Koch 1837) based on maximum likelihood analysis of 112 morphological characters and 1078 base pairs of DNA sequence from the mitochondrial Cytochrome *c* Oxidase Subunit I gene for 53 specimens of the ingroup with outgroup species of *Centruroides* and *Heteroctenus junceus* (Herbst, 1800). Material was deposited in the following collections: Ambrose Monell Cryo Collection (AMCC) at the American Museum of Natural History, New York; Colección Nacional de Arácnidos, Instituto de Biología (CNAN), Universidad Nacional Autónoma de Mexico, Mexico City; California Academy of Sciences (CASENT), San Francisco; Oxford University Museum of Natural History (OUMNH), UK.

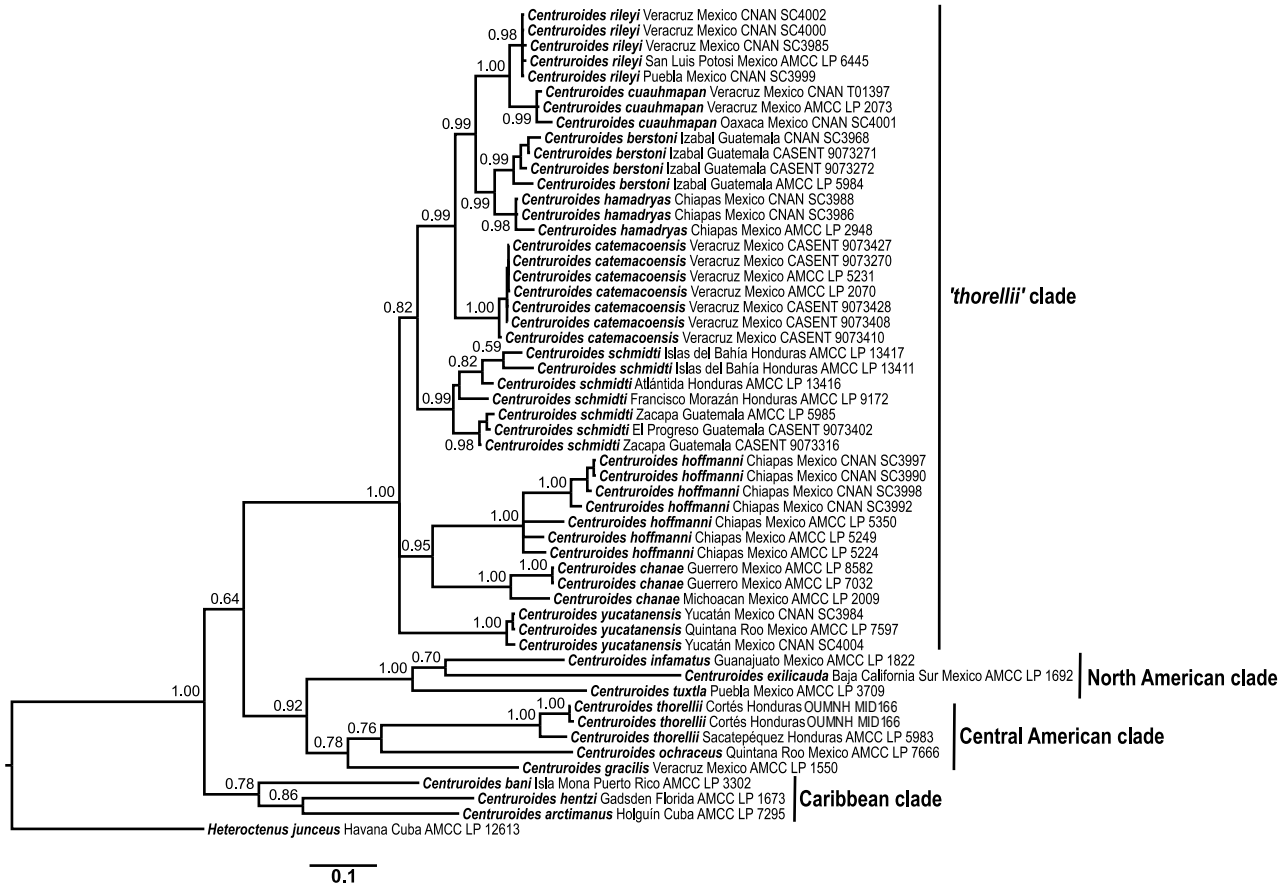

Figure 3. Phylogeny of the arboreal Neotropical '*thorellii*' clade of *Centruroides* Marx, 1890 bark scorpions (Buthidae C.L. Koch 1837) based on Bayesian analysis of 112 morphological characters and 1078 base pairs of DNA sequence from the mitochondrial Cytochrome *c* Oxidase Subunit I gene for 53 specimens of the ingroup with outgroup species of *Centruroides* and *Heteroctenus junceus* (Herbst, 1800). Material was deposited in the following collections: Ambrose Monell Cryo Collection (AMCC) at the American Museum of Natural History, New York; Colección Nacional de Arácnidos, Instituto de Biología (CNAN), Universidad Nacional Autónoma de Mexico, Mexico City; California Academy of Sciences (CASENT), San Francisco; Oxford University Museum of Natural History (OUMNH), UK.

Although this study demonstrates the effectiveness of mini-barcodes in sequencing specimens preserved in suboptimal conditions, several caveats must be taken into consideration.

Mitochondrial genes such as COI are regarded as the gold standard for DNA barcoding as their high mutation rates allow the sorting of specimens to species level with relative ease, low cost, and efficiency [46,47]. However, recent studies demonstrated that short mini-barcodes (<200 bp) perform more poorly than barcodes of medium length (>200 bp), necessitating other lines of evidence to differentiate species [45]. The addition of slow-mutating nuclear genes is necessary to resolve deep basal evolutionary relationships [21,22,27]. The incorporation of both mitochondrial and nuclear genes with differing mutation rates is desirable as it improves the support and stability of nodes.

The ML and BI trees presented here received low support for the internal nodes, most likely due to the absence of a nuclear gene. Successful amplification of nuclear genes proved fruitless, even when attempting to amplify shorter fragments such as the Internal Transcribed Spacer (ITS2, 350 bp) and Histone 3 (H3, 300 bp) [48,49]. The shorter, 125-bp mini-barcode primers would have provided insufficient support for species delimitation in the absence of other lines of evidence. The inclusion and analysis of a morphological character matrix with the COI data allowed an integrative approach to species delimitation in the '*thorellii*' clade.

Table 2. Genetic distances and species delimitation metrics among and within species of the arboreal Neotropical '*thorellii*' clade of *Centruroides* Marx, 1890 bark scorpions (Buthidae C.L. Koch 1837). Definitions modified from Masters et al. (2011): Intra Dist: average pairwise tree distance among species; Inter Dist: average pairwise tree distance within species; Intra/Inter: ratio of Intra Dist to Inter Dist; P ID (Strict): mean probability, with 95% confidence interval (CI), of correct identification of unknown specimen using placement on tree; P ID (Liberal): mean probability, with 95% confidence interval (CI), of correct identification of unknown specimen using BLAST (best sequence alignment), DNA Barcoding (closest genetic distance), or placement on tree; Av (MRCA-tips): mean distance between most recent common ancestor of species and its conspecific members; P (RD): probability that clades have observed degree of distinctiveness; P (AB): probability that clades are reciprocally monophyletic.

Putative Species	Specimens	Closest Species	Intra Dist	Inter Dist	Intra/Inter	P ID (Strict)	P ID (Liberal)	Av (MRCA-Tips)	P (RD)	P (AB)
1: *C. rileyi*	5	**2:** *C. cuauhmapan*	0.007	0.055	0.12	0.85 (0.73, 0.98)	0.97 (0.87, 1.0)	0.003	0.05	0.01
2: *C. cuauhmapan*	3	**1:** *C. rileyi*	0.002	0.055	0.36	0.55 (0.37, 0.73)	0.80 (0.66, 0.95)	0.010	0.19	0.01
3: *C. berstoni*	4	**4:** *C. hamadryas*	0.035	0.075	0.47	0.55 (0.41, 0.70)	0.83 (0.72, 0.94)	0.022	0.93	0.01
4: *C. hamadryas*	3	**3:** *C. berstoni*	0.016	0.075	0.22	0.65 (0.47, 0.82)	0.88 (0.74, 1.0)	0.081	0.13	0.01
5: *C. catemacoensis*	7	**1:** *C. rileyi*	0.007	0.110	0.06	0.92 (0.81, 1.0)	0.98 (0.92, 1.0)	0.010	0.05	5.50×10^{-7}
6: *C. schmidti*	7	**5:** *C. catemacoensis*	0.073	0.161	0.46	0.71 (0.61, 0.82)	0.90 (0.84, 0.96)	0.045	0.59	4.50×10^{-8}
7: *C. hoffmanni*	7	**5:** *C. chanae*	0.069	0.251	0.28	0.81 (0.71, 0.92)	0.93 (0.87, 0.99)	0.05	1.0	1.85×10^{-3}
8: *C. chanae*	3	**9:** *C. schmidti*	0.058	0.251	0.23	0.64 (0.46, 0.81)	0.88 (0.73, 1.0)	0.042	1.0	1.85×10^{-3}
9: *C. yucatanensis*	3	**8:** *C. schmidti*	0.014	0.197	0.07	0.74 (0.57, 0.92)	0.97 (0.82, 1.0)	0.008	0.05	4.20×10^{-6}

Importantly, in most cases, multiple specimens of each species were represented by both partial COI and mini-barcodes, allowing more accurate alignments. Future analyses using mini-barcodes should include additional datasets for species identification if possible [46,50].

Diversification

The complex topography of the Mexican and Central American landscapes together with the ecological specialization of these scorpions are hypothesized to have driven diversification in the '*thorellii*' clade, which appears to display high levels of endemism. The arboreal habits of the clade confer a unique niche safe from predation by larger ground-dwelling scorpion species as well as other ground-dwelling predators [51]. Species such as *C. berstoni*, *C. catemacoensis*, and *C. hamadryas* exhibit very specific temperature, humidity, and substrate preferences [52]. Evidence of population structure among habitats but genetic admixture within habitats suggests these species are not constrained by dispersal within a given habitat but have narrow ecological requirements preventing them from dispersing between habitats.

The analyses identified geographically structured intraspecific genetic variation, despite morphological conservatism. For example, *C. hoffmanni* displayed a genetic structure among specimens collected less than 50 km apart. This species occurs predominantly within the Chiapas Depression, which acts as a corridor for some species and a barrier for others [53]. The results of the species delimitation analyses suggested all individuals of *C. hoffmanni* are conspecific, as genetic differentiation is minimal. The specialized arboreal microhabitat of *C. hoffmanni* suggests dispersal is limited across its broad geographical range, resulting in genetic divergence among populations occupying heterogeneous habitats, from evergreen and broadleaf forests to savannahs and scrub, across the Chiapas Depression.

A similar pattern was apparent with *C. schmidti*, in which divergence was evident among specimens from Guatemala and Honduras. Localities within the neighboring El Progresso and Zacapa departments of Guatemala share contiguous pine savannah and thorn forests. Localities within Honduras originated from Atlántida and Islas del Bahía, tropical coastlines with offshore islands characterized by broadleaf forests which receive high rainfall.

A third example is provided by *C. chanae*, in which divergence was evident between specimens separated by the Balsas Depression, an arid basin covering part of southwestern Guerrero and most of northwestern Michoacán in southern Mexico, which represents a barrier for other arachnid species [54–57]. Future studies should sample the entire ranges of *C. chanae*, *C. hoffmanni*, and *C. schmidti* to better understand the population structure within these species and investigate the possibility of additional cryptic species.

In contrast to *C. chanae*, *C. hoffmanni*, and *C. schmidti*, little genetic divergence was evident among specimens of *C. rileyi* distributed over a large area of northeastern Mexico, in the states of San Luis Potosí and Tamaulipas, suggesting unrestricted gene flow among populations. This may be due to the absence of barriers to dispersal across the homogenous Tamaulipan mezquital, a subhumid xeric shrubland biome which encompasses most of the lowlands of both states [58].

5. Conclusions

Systematics has reached a critical point in the 21st century where the rate of species description must outpace the decline of biodiversity [46]. Specimens must be rapidly sorted to the species level to infer large-scale biodiversity patterns. Such baseline work is essential to determine changes in species richness caused by climate change and habitat destruction. Luckily, vast numbers of specimens, including many undescribed species, are already housed within natural history collections; the challenge comes in developing faster, cheaper, and more efficient molecular sorting methods to harness data for their delimitation and identification, regardless of the age or preservation of the specimen [47].

Mini-barcodes have been lauded for species-level identification in degraded museum material due to their low cost on short-read sequencing platforms (e.g., Illumina) and their similar performance to complete barcodes [47]. This study presents the first use of mini-barcodes to delimit arachnid species from museum material and highlights the potential of mini-barcodes for species delimitation in arthropods more broadly. With roughly 28 million species remaining to be described [59], mini-barcodes provide another tool in the taxonomist's toolkit to assist with documenting the world's biodiversity while the opportunity remains.

Author Contributions: Conceptualization, L.A.E. and A.M.G.; methodology, L.A.E., L.P. and A.M.G.; software, L.A.E.; validation, L.A.E. and L.P.; formal analysis, A.M.G.; investigation, A.M.G. and L.A.E.; resources, L.A.E. and L.P.; data curation, A.M.G. and L.P.; writing—original draft preparation, A.M.G.; writing—review and editing, A.M.G., L.A.E. and L.P.; visualization, A.M.G., L.A.E. and L.P.; supervision, L.A.E. and L.P.; project administration, L.A.E.; funding acquisition, A.M.G., L.A.E. and L.P. All authors have read and agreed to the published version of the manuscript.

Funding: The research presented herein comprised part of the MSc thesis of A.M. at San Francisco State University and the CAS, partially supported by a grant from the Vincent Roth Fund for Systematic Research of the American Arachnological Society and a Collections Study Grant from the AMNH. Some data presented herein emanated from the PhD dissertation of L.A.E. at the City University of New York (CUNY) and the AMNH, supported by a U.S. National Science Foundation (NSF) GK-12 Fellowship, a CUNY/NSF AGEP Grant, a CUNY Presidential Fellowship, a CUNY College Now Fellowship, and an NSF Postdoctoral Fellowship (1003087). Additional funding for this research was provided by a grant from the Theodore Roosevelt Memorial Fund of the AMNH to L.A.E.; an Ernst Mayr Award from the Museum of Comparative Zoology, Harvard University, to L.A.E.; an NSF Doctoral Dissertation Improvement Grant (DEB 0910147) to L.P. and L.A.E.; an NSF grant (DEB 0413453) to L.P., and a grant from the Richard Lounsbery Foundation to L.P.

Institutional Review Board Statement: Ethical review and approval were waived for this study, due to experimentation on nonliving invertebrate museum specimens.

Informed Consent Statement: Not applicable.

Data Availability Statement: The data presented in this study are openly available in the Dryad digital repository (datadryad.org) at (doi:10.5061/dryad.fttdz08t2; accessed on 18 June 2021).

Acknowledgments: We thank the following for assisting with fieldwork or donating material used in the study: L. Allen, A.J. Ballesteros, D. Barrales-Alcalá, M.A. Barrios-Izás, P. Berea, G. Bonilla, J.L. Castelo, D. Chibras, M. Cordóva, M. Escalante, T. Gearheart, E. González-Santillán, J. Gorneau, J.H. Huff, A. Jaimes, M.K. Lippey, S. Longhorn, R. Monjaraz-Ruedas, H. Montaño, G. Montiel-Parra, D. Ortíz, R. Paredes, J. Ponce-Saavedra, M. Ramírez, M.E. Soleglad, A. Tietz, A. Valdez, M. van Dam, G. Villegas, C. Víquez, and H. Yamaguti; R. Coates Lutes for use of the Los Tuxtlas Field Station; E.S. Volschenk for providing unpublished morphological characters; D. Casellato, P. Rubi, and T. Sharma for generating some of the DNA sequence data at the AMNH; A. Lam, M. van Dam, L. Bonomo, and S.F. Loria for assistance with DNA sequencing and phylogenetic analysis at the CAS; P. Colmenares for logistical support with collections at the AMNH, and four reviewers for constructive comments on a previous draft of the manuscript.

Conflicts of Interest: The authors declare no conflict of interest.

Appendix A

Specimens and tissue samples from which DNA was extracted and morphology was examined for phylogenetic analysis of the arboreal Neotropical '*thorellii*' clade of *Centruroides* Marx, 1890 bark scorpions (Buthidae C.L. Koch 1837) and outgroup species of *Centruroides* and *Heteroctenus junceus* (Herbst, 1800). Material was deposited in the following collections: Ambrose Monell Cryo Collection (AMCC) at the American Museum of Natural History, New York; Colección Nacional de Arácnidos, Instituto de Biología (CNAN), Universidad Nacional Autónoma de México, Mexico City; California Academy of Sciences (CASENT), San Francisco; Oxford University Museum of Natural History (OUMNH), UK.

Outgroup

***Centruroides arctimanus* Armas, 1976: CUBA:** *Holguín*: Município Holguín: 20°53′32.8″ N 76°17′04.7″ W, 3.x.2007, A. Tietz, 2 juv. (AMCC [LP 7295]).

***Centruroides bani* Armas and Marcano Fondeur, 1987: U.S.A.:** *Puerto Rico:* Isla Mona, road between Sardiniera and airport: 18°03′48.4″ N 67°53′14.3″ W, 18.x.2009, L.A. Esposito and H. Yamaguti, 1 ♂ (AMCC [LP 3302]).

***Centruroides exilicauda* (Wood, 1863): MEXICO:** *Baja California Sur:* Município Los Cabos: Cabo San Lucas, 15 mi. E, 12°53′23″ N 109°54′56″ W, 1.vi.1999, M.E. Soleglad, 1 ♂ (AMCC [LP 1692]).

***Centruroides gracilis* (Latreille, 1804): MEXICO:** *Veracruz*: Município Actopan: Puente Nacional, Los Idolos, 19°25′44.9″ N 96°32′12.4″ W, 5.v.2006, O.F. Francke, P. Berea, and A. Ballesteros, 1 ex. (AMCC [LP 1550]).

***Centruroides hentzi* (Banks, 1900): U.S.A.:** *Florida*: Gadsden County, 16.v.2000, T. Gearheart, 1 ♂ (AMCC [LP 1673]).

***Centruroides infamatus* (C.L. Koch, 1844): MEXICO:** *Guanajuato*: Município Acámbaro: 2 km N Pueblo San Luis de los Agustinos, 20°12′27.9″ N 100°41′22.2″ W, 25.III.2006, O.F. Francke, A. Valdez, G. Villegas, H. Montaño, and C. Santibañez, 2 ♂ (AMCC [LP 1822]).

***Centruroides ochraceus* (Pocock, 1898): MEXICO:** *Quintana Roo*: Município Benito Juárez: Puerto Morelos, Botanical Gardens, 20°50′42.1″ N 86°54′12.9″ W, 4.VIII.2007, G. Montiel and R. Paredes, 1 subad. ♂ (AMCC [LP 7666]).

***Centruroides thorellii* (Kraepelin, 1891): GUATEMALA:** *Sacatepéquez*: Município Antigua: Parque Senderos de Alux, 15–20 km W of Guatemala City, 14°36′38.9″ N 90°38′20.8″ W, 30.VII.2008, J. Huff, C. Víquez, E. Agreda, and D. Ortíz, 1 ♀, 4 ex. (AMCC [LP 5983]). **HONDURAS:** *Cortés*: Município San Pedro Sula: Parque Nacional Cusuco, Cantilles Site, CA2 (Transect 2, subsite 3), 15°30′48″ N 88°14′23″ W, M. D'Sousa, K. Sagastume, and S. Longhorn, 2 ♀ (OUMNH [MID166]).

***Centruroides tuxtla* Armas, 1999: MEXICO:** *Chiapas*: Município Suchiapa: La Vuelta del Alacran, 4.8 km from km 27 on road from Ocozocuautla to Villa Flores, 16°32′35.2″ N 93°12′09.8″ W, x.2004, R. Paredes, O.F. Francke, and G. Villegas, 1 ♂, 1 ♀ (AMCC [LP 3709]).

***Heteroctenus junceus* (Herbst, 1800): CUBA:** *Guantánamo*: Município Baracoa: Alejandro Humboldt National Park, near El Yunque de Baracoa, 20°20′42.1″ N 74°33′59.1″ W, 370 m, 5.iv.2012, CarBio team, 1 ♂ (AMCC [LP 12613]).

Ingroup

***Centruroides berstoni* Goodman et al., 2021: GUATEMALA:** *Departamento Izabal*: Município Livingston: Biotopo Chocón Machacas, 15°44′05.3″ N 88°54′57.2″ W, 15 m, 25.ix.2019, A.M. Goodman, 8 ♂, 1 ♀, 1 juv. ♂ (CASENT 9073271); Río Dulce, Hotel Tijax, 15°40′12.2″ N 89°00′27″ W, 49 m, 8.vii.2006, J. Huff, C. Víquez, and D. Ortíz, collected along trails through old secondary growth tropical forest using UV at night, 1 ♂ (AMCC [LP 5984]); 15°39′51.2″ N 89°00′14.6″ W, 17 m, 24.ix.2019, A.M. Goodman, collected along gravel road of Hacienda Tijax Parking Lot, flanked by bamboo groves and live fencing, 1 ♂ (CASENT 9073272); 15°44′05.3″ N 88°54′57.2″ W, 15 m, 25.ix.2019, A.M. Goodman, 8 ♂, 1 ♀, 1 juv. ♂ (CASENT 9073271). Município Morales: Morales, Finca Fiymeza, Sendero Anfibio, 15°24′24.1″ N 88°41′46.8″ W, 595 m, 17.viii.2017, D. Barrales and R. Monjaraz, 1 juv. ♀ (CNAN SC3968).

***Centruroides catemacoensis* Goodman et al., 2021: MEXICO:** *Veracruz*: Município Catemaco: Estacion Biología Los Tuxtlas, UNAM, 18°35′05.6″ N 95°04′29.9″ W, 134 m, 26.viii.2005, O.F. Francke, M. Córdova, A. Jaimes, A. Valdez, and H. Montaño, 1 ♂ (AMCC [LP 5231]); 18°34′54″ N 95°04′54.6″ W, 134 m, 19.vii.2002, J. Ponce and O.F. Francke, 1 ♀ (AMCC [LP 2070]), 74–416 m, 17.vii–25.vii.2018, A.M. Goodman, J. Gorneau, and M.K. Lippey, 2 ♂ (CASENT 9073270, 9073427), 4 juv. ♀ (CASENT 9073408, 9073410, 9073428).

***Centruroides chanae* Goodman et al., 2021: MEXICO:** *Guerrero*: Município Copala: Microondas Fogos, 16°33′59.5″ N 98°53′18.1″ W, 103 m, 22.vi.2007, O.F. Francke, M. Es-

calante, H. Montaño, and A. Ballesteros, 1 ♂ (AMCC [LP 7032]), 1 ♀ (AMCC [LP 8582]). *Michoacán*: Município Aquila: Faro de Bucerias, 18°21′08.3″ N 103°30′20.9″ W, 13 m, 10.iii.2002, J. Ponce, low deciduous forest, 3 ♂ (CNAN SC4005); 18°35′50.5″ N 103°30′04.3″ W, 221 m, 14.iv.2002, J. Ponce and E. González, low deciduous forest, 1 ♂ (AMCC [LP 2009]).

Centruroides cuauhmapan **Goodman et al., 2021: MEXICO:** *Oaxaca*: Município San Juan Bautista Tuxtepec: 17 km from San Juan Bautista Tuxtepec, Cerro del Oro Dam, 17°59′55″ N 96°15′47.2″ W, 74 m, 23.v.1990, E. Barrera and A. Cadena, 1 ♂ (CNAN SC4001). *Veracruz*: Município Amatlán de los Reyes: Cañada Blanca, 18°55′43.5″ N 96°51′26″ W, 555 m, 18.vii.2002, E. González, found in coffee plantation in lowland rainforest, collected at night with UV light, 1 ♂ (AMCC [LP 2073]). Município Actopan: Los Idolos, 19°25′44.9″ N 96°32′12.4″ W, 112 m, 5.v.2006, O.F. Francke, P. Berea, and A.J. Ballesteros, collected with UV detection, 2 ♂paratypes (CNAN T01397).

Centruroides hamadryas **Goodman et al., 2021: MEXICO:** *Chiapas*: Municipío Ocosingo: La Galleta, 2 km SE of Frontera Corozal, 16°48′12.7″ N 90°52′11.1″ W, 132–150 m, 28.iv.2004, R. Paredes and J.L. Castelo, collected with UV light detection, 2 ♂ (AMCC [LP 2948]); 16°49′55″ N 90°56′08″ W, 146 m, 7.iv.2005, A. Valdez, O.F. Francke, and A. Ballesteros, collected at night with UV lamp, 1 juv. ♂ (CNAN SC3986); 16°48′18.5″ N 90°54′25″ W, 114 m, 28.iv.2005, A. Valdez, O.F. Francke, and A. Ballesteros, urban area towards blue water bridge, collected with UV light detection, 2 ♂, 1 ♀, 1 juv. ♂, 1 juv. ♀ (CNAN SC3988).

Centruroides hoffmanni **Armas, 1996: MEXICO:** *Chiapas*: Município Ángel Albino Corzo: 8 km from Siltepec, 18°48′33″ N 92°40′30.6″ W, 663 m, 17.viii.2007, C. Mayorga, G. Ortega, and L. Cervantes, 1 juv. ♀ (CNAN SC3990). Município Comitan: Parque Nacional Lagunas de Montebelo, 16°17′17″ N 91°56′16″ W, 1473 m, 3.ix.2005, O.F. Francke, M. Córdova, A. Jaimes, A. Valdez, and H. Montaño, 1 juv. ♂ (CNAN SC3992). Município La Concordia: Villa Corzo La Tigrilla, San Julián, Revolución Mexicana, 16°00′00″ N 92°50′47″ W, 544 m, 17.iii.2007, C. Mayorga, G. Ortega, and L. Cervantes; 1 ♂, 1 ♀ (CNAN SC3998). Município Tuxtla Gutiérrez: Las Delicias, 16°45′31.1″ N 93°06′26.4″ W, 529 m, 2.iii.2005, O.F. Francke, M. Córdova, A. Jaimes, A. Valdez, and H. Montaño, 1 ♀ (AMCC [LP 5224]); Gutiérrez, San Julián, Revolución Mexicana, 16°11′41″ N 93°01′16″ W, 544 m, 16.iii.2007, G. Ortega and A. Cervantes, 2 ♂, 3 ♀ (CNAN SC3997). Município Tzimol: Carretera [Hwy] Comitán–Tzimol Santa Rosa, 16°11′03.4″ N 92°16′59.3″ W, 632–730 m, 2.ix.2005, O.F. Francke, M. Córdova, A. Jaimes, A. Valdez, and H. Montaño, 1 ♂, 1 ♀ (AMCC [LP 5249]). Município Villaflores: Reserva de La Biosfera La Sepultura, 1 km SE of Ejido California, 16°15′14.2″ N 93°35′46.4″ W, 1009–1132 m, 30.viii.2005, O.F. Francke, M. Córdova, A. Jaimes, A. Valdez, and H. Montaño, 1 ♂ (AMCC [LP 5350]).

Centruroides rileyi **Sissom, 1995: MEXICO:** *Puebla*: Município Cuetzalan el Progreso: Cuetzalan, Santiago Yancuitlalpan, 18°54′42.2″ N 98°35′15.3″ W, 2554 m, 19.v.1995, G. Oclogaig Barrzia, juvs (CNAN SC3999). *San Luis Potosí*: Município Axtlan de Terrazas: Axtlan de Terrazas, 21°25′34.9″ N 98°52′42″ W, 100 m, 28.iv.2006, O.F. Francke, A. Valdez, G. Villegas, and R. Paredes, 1 ♂ (AMCC [LP 6445]). *Veracruz*: Município Paplanta: Papantla 20°27′24.1″ N 97°18′56.1″ W, 2197 m, iii.2000, J.L. Castelo, 1 ♂ (CNAN SC4000). Município Tamiahua: Moralillo, Cerro Azul, 21°11′03.8″ N 97°44′49.6″ W, 153 m, 27.ii.2007, E. Barrera and L. Cervantes, 2 ♀ (CNAN SC3985), 1 juv. ♀ (CNAN SC4002).

Centruroides schmidti **Sissom, 1995: GUATEMALA:** *Departamento El Progreso*: Município Rio Hondo: San Francisco Zapotitlan: Finca El Olvido, Las Minas, 15°02′04.8″ N 89°52′26.7″ W, 1214 m, 18.ix.2019, A.M. Goodman, L.A. Esposito, and L. Allen, 5 ♀, 1 juv. ♂, 1 juv. ♀ (CASENT 9073402). *Departamento Zacapa*: Município Rio Hondo: Bosque Pino, Guadalupe, Manta de Golpeo, 14°58′04.7″ N 89°24′47″ W, 751 m, 20.ix.2019, A.M. Goodman, M. Barrios, and M. van Dam, UV hand collection, found on oak and pine trees, 2–3 m high, 7 ♂, 1 ♀, 1 juv. ♂, 1 juv. ♀ (CASENT

9073278); Aldea Casas de Pinto, near turnoff for Zacapa at Rio Hondo, 15°01′38.2″ N 89°36′57.2″ W, 77 m, 13.vii.2006, J.H. Huff, semi-arid region with scrub forest and cacti, collected under rocks in shaded areas and at night using UV, 1 ad. (AMCC [LP 5985]). **HONDURAS:** *Departamento Atlántida*: Município La Ceiba: Parque Nacional Pico Bonito, Pico Bonito, trails from Visitor Centre and park entrance, 14°43′30.6″ N 86°44′11.5″ W, 184 m, 30.viii.2013, S. Longhorn, dense wet lowland tropical forest near large river, sweeping and beating, may have been on or under wood, day search, 1 juv. ♂ (AMCC [LP 13416]). *Departmento Francisco Morazán*: Município San Antonio de Oriente: E.A.P. Zamorano, Monte Redondo, Acuacultura, 13°39′59.6″ N 86°59′21″ W, 773 m, 23.ix.2008, C. Víquez, UV at night, 1 ♀ (AMCC [LP 9172]). *Departamento Islas de la Bahía*: Município Roatán: Cayos Cochinos, Cayos Menor, forest trails, 15°57′26.9″ N 86°30′03.3″ W, 101 m, 2.viii.2012, S. Longhorn, scrub oak forest, 1 ♀ (AMCC [LP 13411]); Isla Utila, 16°06′22.1″ N 86°54′08.1″ W, 12 m, 21.vii.2012, S. Longhorn, scrub forest/wet savannah, 1 ♀ (AMCC LP [13417]).

Centruroides yucatanensis **Goodman et al., 2021: MEXICO:** *Quintana Roo*: Município Benito Juarez: Puerto Morelos, Jardin Botanico Alfredo Barrera, 20°50′42.1″ N 86°54′12.9″ W, 38 m, 4.vii.2007, G. Montiel, R. Paredes, M. Ramírez, D. Chibras, and G. Bonilla, 1 ♂ (AMCC [LP 7597]), 2 juv. ♂ (CNAN SC3984). *Yucatán*: Município Felipe Carrillo Puerto: Cenote Chac-ha, 3.5 km N and 3 km E of Kalacmul, 20°04′40.3″ N 88°08′27.9″ W, 23 m, 9.vii.2007, R. Paredes, D. Chibras, and G. Montiel, 1 ♀ (CNAN SC4004).

Appendix B

Tissue samples, base pair lengths, localities, and GenBank accession codes of DNA sequences from the mitochondrial Cytochrome *c* Oxidase Subunit I gene used for phylogenetic analysis of the arboreal Neotropical '*thorellii*' clade of *Centruroides* Marx, 1890 bark scorpions (Buthidae C.L. Koch 1837) and outgroup species of *Centruroides* and *Heteroctenus junceus* (Herbst, 1800). Material was deposited in the following collections: Ambrose Monell Cryo Collection (AMCC) at the American Museum of Natural History, New York; Colección Nacional de Arácnidos, Instituto de Biología (CNAN), Universidad Nacional Autónoma de México, Mexico City; California Academy of Sciences (CASENT), San Francisco; Oxford University Museum of Natural History (OUMNH), UK. Sequences less than 150 bp in length were deposited in the Dryad digital repository (doi:10.5061/dryad.fttdz08t2). Sequences of 127–134 bp are mini-barcodes, 430–659 bp are partial COI, and sequences of 1078 bp are complete COI.

Species	Coll. Number	Locality	Length	GenBank Code
Outgroup				
H. junceus	AMCC [LP 12613]	Cuba: Guantánamo: Humboldt N. P.	1078	KY982192.1
C. bani	AMCC [LP 3302]	Puerto Rico: Isla Mona	1078	MK479164.1
C. exilicauda	AMCC [LP 1692]	Mexico: Baja California Sur: Cabo San Lucas	1078	KY982179.1
C. gracilis	AMCC [LP 1550]	Mexico: Veracruz: Los Idolos	1078	MK479175.1
C. hentzi	AMCC [LP 1673]	U.S.: Florida: Gadsden Co.	1078	MK479177.1
C. infamatus	AMCC [LP 1822]	Mexico: Guanajuato: Acámbaro	1078	KY982181.1
C. ochraceus	AMCC [LP 7666]	Mexico: Morelos: Puerto Morelos Bot. Gard.	1078	MK479194.1
C. thorellii	AMCC [LP 5983]	Guatemala: Sacatepéquez: Parque Alux	1078	MK479208.1
	OUMNH [MID166]	Honduras: Cortés: San Pedro Sula	642	MZ366335
			658	MZ366336
C. tuxtla	AMCC [LP 3709]	Mexico: Chiapas: La Vuelta de Alacran	1078	MK479209.1
Ingroup				
C. berstoni	CASENT 9073271	Guatemala: Izabal: Biotopo Chocón Machacas	430	MZ366346
	CASENT 9073272	Guatemala: Izabal: Hotel Tijax	621	MZ366345
	CNAN SC3968	Guatemala: Izabal: Morelos	658	MZ366344

Appendix B
Cont.

Species	Coll. Number	Locality	Length	GenBank Code
Ingroup				
C. catemacoensis	AMCC [LP 2070]	Mexico: Veracruz: Los Tuxtlas	1078	MZ429054
	AMCC [LP 5231]		1078	MZ429055
	CASENT 9073270		659	MZ366343
	CASENT 9073408		648	MZ366342
	CASENT 9073410		658	MZ366341
	CASENT 9073427		659	MZ366340
	CASENT 9073428		648	MZ366339
C. chanae	AMCC [LP 2009]	Mexico: Michoacán: Faro de Bucerias	1078	MZ429056
	AMCC [LP 7032]		1078	MZ429057
	AMCC [LP 8582]	Mexico: Guerrero: Microondas Fogos	1078	MZ429058
C. cuauhmapan	AMCC [LP 2073]	Mexico: Veracruz: Cañada Blanca	1078	MZ429059
	CNAN SC4001	Mexico: Oaxaca: Cerro del Oro	40	-
	CNAN T01397	Mexico: Veracruz: Los Idolos	127	-
C. hamadryas	AMCC [LP 2948]	Mexico: Chiapas: La Galleta	1078	MZ429060
	CNAN SC3986		127	-
	CNAN SC3988		127	-
C. hoffmanni	AMCC [LP 5224]	Mexico: Chiapas: Las Delicias	1078	MZ429061
	AMCC [LP 5249]	Mexico: Chiapas: Santa Rosa	1078	MZ429062
	AMCC [LP 5350]	Mexico: Chiapas: Res. Biosfera Sepultura	1078	MK479178.1
	CNAN SC3990	Mexico: Chiapas: Siltepec	134	-
	CNAN SC3992	Mexico: Chiapas: P. N. Lagunas de Montebelo	137	-
	CNAN SC3997	Mexico: Chiapas: Gutierrez	134	-
	CNAN SC3998	Mexico: Chiapas: Villa Corzo	138	-
C. rileyi	AMCC [LP 6445]	Mexico: San Luis Potosí: Axtlan de Terrazas	1078	KY982183.1
	CNAN SC3985	Mexico: Veracruz: Cerro Azul	127	-
	CNAN SC3999	Mexico: Puebla: Cuetzalan	127	-
	CNAN SC4000	Mexico: Veracruz: Papantla	127	-
	CNAN SC4002	Mexico: Veracruz: Cerro Azul	127	-
C. schmidti	AMCC [LP 13416]	Honduras: Atlántida: Pico Bonito	127	-
	AMCC [LP 13411]	Honduras: Isla del Bahía: Cayos Menor	1078	MZ429064
	AMCC [LP 13417]		1078	MZ429065
	AMCC [LP 5985]	Guatemala: Zacapa: Aldea casas de Pinto	1078	MZ429063
	AMCC [LP 9172]	Honduras: Francisco Morazán: E.A.P. Zamorano	1078	KY982184.1
	CASENT 9073316	Guatemala: Zacapa: Guadalupe	606	MZ366338
	CASENT 9073402	Guatemala: Zacapa: Las Minas	620	MZ366337
C. yucatanensis	AMCC [LP 7597]	Mexico: Quintana Roo: Puerto Morelos	1078	MK479201.1
	CNAN SC3984		127	-
	CNAN SC4004	Mexico: Yucatán: Cenote Chac-ha	127	-

Appendix C

Morphological characters and character states used in phylogenetic analysis of the arboreal Neotropical '*thorellii*' clade of *Centruroides* Marx, 1890 bark scorpions (Buthidae C.L. Koch 1837) and outgroup species of *Centruroides* and *Heteroctenus junceus* (Herbst, 1800). Morphological terminology follows Hjelle (1990) and Sissom (1990), except for carapace and metasomal carination, which follows Vachon (1952); trichobothria, which follows Vachon (1974); tergite and pedipalp carination, which follows Prendini (2000); book lung anatomy, which follows Kamenz and Prendini (2008); and ovariuterine anatomy, which follows Volschenk et al. (2008).

Carapace

1. Lateral ocular carinae: 0, present, distinct; 1, reduced to several granules; 2, absent (E.S. Volschenk and L. Prendini, unpublished data; Esposito et al. 2017, 2018).
2. Centrolateral carinae: 0, present; 1, absent (E.S. Volschenk and L. Prendini, unpublished data; Esposito et al., 2017, 2018).
3. Anterior centrosubmedian carinae: 0, present; 1, absent (E.S. Volschenk and L. Prendini, unpublished data; Esposito et al., 2017, 2018).
4. Posterior centrosubmedian carinae: 0, present; 1, absent (E.S. Volschenk and L. Prendini, unpublished data; Esposito et al., 2017, 2018).

5. Anteromedian notch: 0, present; 1, absent (Esposito, 2011).
6. Surface granulation density: 0, smooth; 1, sparsely granular; 2, densely granular medially; 3, densely granular throughout (Esposito, 2011).
7. Surface granulation texture: 0, weakly granular, shagreened; 1, large, rounded granules; 2, large, conical granules (Esposito, 2011).
8. Anterior median ocular sulcus: 0, absent; 1, wide; 2, narrow, deep (Esposito, 2011).
9. Median ocular sulcus: 0, absent; 1, wide; 2, narrow, deep (Esposito, 2011).
10. Posteromedian sulcus: 0, absent; 1, wide; 2, narrow, deep (Esposito, 2011).
11. Posteromarginal sulci: 0, absent; 1, present (Esposito, 2011).
12. Posterolateral sulci: 0, absent; 1, present (Esposito, 2011).
13. Anterior margin, carina: 0, absent; 1, smooth; 2, granular (Esposito, 2011).
14. Lateral margins, carina: 0, absent; 1, smooth; 2, granular (Esposito, 2011).
15. Posterior margin, carina between posterior centrosubmedian carinae: 0, absent; 1, smooth; 2, granular (Esposito, 2011).

Pedipalps

16. Chela prodorsal carina: 0, granular; 1, smooth; 2, absent (E.S. Volschenk and L. Prendini, unpublished data; Esposito, 2011; Esposito et al., 2017, 2018).
17. Chela retrodorsal carina: 0, granular; 1, smooth; 2, absent (E.S. Volschenk and L. Prendini, unpublished data; Esposito, 2011).
18. Chela retromedian carinae: 0, granular; 1, smooth; 2, absent; 3, vestigial, reduced to several sparse granules; ?, unknown (E.S. Volschenk and L. Prendini, unpublished data; Esposito, 2011; Esposito et al., 2017, 2018).
19. Chela retroventral accessory carina: 0, complete; 1, reduced; 2, absent (E.S. Volschenk and L. Prendini, unpublished data; Esposito, 2011).
20. Chela retroventral carinae: 0, granular; 1, smooth; ?, unknown (Esposito, 2011; Esposito et al., 2017, 2018).
21. Chela retrodorsal accessory carinae: 0, present; 1, absent (Esposito, 2011; Esposito et al., 2017, 2018).
22. Chela prodorsal accessory carinae: 0, present; 1, absent (Esposito, 2011; Esposito et al., 2017, 2018).
23. Patella dorsomedian carina: 0, present; 1, absent (Esposito, 2011).
24. Femur retromedian carinae: 0, small granules; 1, large, conical granules (Esposito, 2011).
25. Fixed finger, number of median denticle subrows: 0, eight; 1, nine; 2, ten or more; 3, seven plus fused proximal subrow; 4, six plus fused proximal subrow (Esposito, 2011; Esposito et al., 2017, 2018).
26. Fixed and movable fingers, supernumary granules; 0, absent; 1, present (Soleglad and Fet, 2003; Esposito, 2011; Esposito et al., 2017, 2018).
27. Movable finger, number of median denticle subrows: 0, eight; 1, nine; 2, eleven; 3, thirteen or more; 4, seven plus fused proximal subrow (Soleglad and Fet, 2003; Prendini, 2004; Esposito, 2011; Esposito et al., 2017, 2018).
28. Chela shape (♂): 0, incrassate (bulbous or swollen); 1, slender (Prendini, 2001, 2004; Esposito, 2011; Esposito et al., 2017, 2018).
29. Chela shape (♀): 0, incrassate (bulbous or swollen); 1, slender (Prendini, 2001; Esposito, 2011; Esposito et al., 2017, 2018).
30. Chela movable finger, proximal lobe (♂): 0, present; 1, absent (Prendini, 2001; Esposito, 2011; Esposito et al., 2017, 2018).
31. Patella prolateral surface, setation: 0, long, dense setae; 1, short, sparse setae (E.S. Volschenk and L. Prendini, unpublished data; Esposito, 2011).

Legs

32. Leg I, tarsal setation: 0, short, dense setae; 1, long, dense setae; 2, sparse setae (E.S. Volschenk and L. Prendini, unpublished data; Esposito, 2011; Esposito et al., 2017, 2018).
33. Leg IV, tarsal setation: 0, short, dense setae; 1, long, dense setae; 2, sparse setae (Esposito, 2011; Esposito et al., 2017, 2018).
34. Legs I–IV, trochanter lateral margin carina: 0, absent; 1, smooth; 2, granular (Esposito, 2011).
35. Telotarsal ungues: 0, long, slightly curved; 1, hooked (Esposito, 2011).

Pectines

36. Pectinal tooth shape: 0, elongate; 1, rounded, spade-like (Esposito, 2011; Esposito et al., 2017, 2018).
37. Proximal teeth, nodules on dorsal surface: 0, one; 1, multiple; 2, absent (Esposito, 2011; Esposito et al., 2017, 2018).
38. Dorsal fulcra: 0, present; 1, reduced (Esposito, 2011).
39. Tympanum-like expansion between lamellae and teeth: 0, absent; 1, present (Esposito, 2011).
40. Proximal fulcra, setal count: 0, one; 1, two; 2, three; 3, four; 4, six or more; 5, none; ?, unknown. (Esposito, 2011; Esposito et al., 2017, 2018).
41. Pectinal plate anterior margin, sulcus (♂): 0, present; 1, absent (Esposito, 2011; Esposito et al., 2017, 2018).
42. Pectinal plate, posterior margin (♂): 0, straight; 1, convex; 2, concave (Esposito, 2011; Esposito et al., 2017, 2018).
43. Median pectinal plate depression (♂): 0, present; 1, absent (Esposito, 2011; Esposito et al., 2017, 2018).
44. Lateral pectinal plate depression (♂): 0, present; 1, absent (Esposito, 2011).
45. Pectinal plate shape (♂): 0, square; 1, rectangular; 2, trapezoidal (Esposito, 2011).
46. Pectinal plate anterior margin, sulcus (♀): 0, present; 1, absent; ?, unknown (Esposito, 2011).
47. Pectinal plate posterior margin (♀): 0, straight; 1, slightly convex; 2, prominently rounded; 3, concave; ?, unknown (Esposito, 2011).
48. Pectinal plate depressions (♀): 0, absent; 1, single wide median depression; 2, paired lateral depressions; 3, single small, deep median depression (pinhole); ?, unknown (Esposito, 2011).

Sternites

49. Sternite VI, ventromedian carina: 0, absent; 1, granular; 2, smooth (E.S. Volschenk and L. Prendini, unpublished data; Esposito, 2011; Esposito et al., 2017, 2018).
50. Sternite V, setation (♂): 0, absent; 1, present, setal base not situated in pits (surface smooth); 2, present, setal base situated in pits (surface punctate) (Esposito, 2011).
51. Sternite VI, ventrolateral carinae: 0, absent; 1, reduced to single granule; 2, present, more than one granule (E.S. Volschenk and L. Prendini, unpublished data; Esposito, 2011; Esposito et al., 2017, 2018).

Tergites

52. Tergites III–VI, dorsolateral carinae: 0, present; 1, absent (E.S. Volschenk and L. Prendini, unpublished data; Esposito, 2011; Esposito et al., 2017, 2018).
53. Tergites III–VI, dorsosubmedian carinae: 0, absent; 1, vestigial; 2, distinct (Prendini, 2004; Esposito, 2011; Esposito et al., 2017, 2018).
54. Tergite VII, median carina: 0, narrow, granular carina; 1, broad, granular carina; 2, broad, smooth carina; 3, vestigial (E.S. Volschenk and L. Prendini, unpublished data; Esposito, 2011; Esposito et al., 2017, 2018).

Metasoma

55. Segment II, median lateral carinae: 0, complete; 1, posteriorly restricted; 2, absent (Esposito, 2011; Esposito et al., 2017, 2018).
56. Segment III, median lateral carinae: 0, complete; 1, posteriorly restricted; 2, absent (Esposito, 2011; Esposito et al., 2017, 2018).
57. Segment III, dorsolateral carinae, posterior granules: 0, similar to preceding granules; 1, larger than preceding granules, acuminate (E.S. Volschenk and L. Prendini, unpublished data; Esposito, 2011; Esposito et al., 2017, 2018).
58. Segment IV, median lateral carinae: 0, absent or obsolete; 1, present (Esposito, 2011; Esposito et al., 2017, 2018).
59. Segment V, posterior margin (anal rim) granulation: 0, present; 1, absent (Esposito, 2011; Esposito et al., 2017, 2018).
60. Segment V, dorsolateral carinae: 0, present; 1, absent (Esposito, 2011; Esposito et al., 2017, 2018).
61. Segment V, median lateral carinae: 0, present; 1, absent (Esposito 2011; Esposito et al., 2017, 2018).
62. Segment V, ventrolateral carinae: 0, present; 1, absent; ?, unknown (Esposito, 2011).
63. Segment V, ventromedian carinae: 0, absent or obsolete; 1, present (Esposito, 2011; Esposito et al., 2017, 2018)
64. Segment V, ventrosubmedian carinae: 0, absent or obsolete; 1, present (Esposito, 2011; Esposito et al., 2017, 2018).
65. Segment V, ratio of segment length to width (♂): 0, slightly elongated, length less than 2x width; 1, moderately elongated, length 2.5–3x width; 2, markedly elongated, length more than 3x width (Esposito, 2011; Esposito et al., 2017, 2018).
66. Segments I–IV, width: 0, narrowing posteriorly, segment I slightly wider than IV; 1, slightly widening posteriorly, segment I slightly narrower than IV; 2, markedly widening posteriorly, segment I much narrower than IV (Esposito, 2011; Esposito et al., 2017, 2018).
67. Metasoma length relative to length of prosoma and mesosoma (♂): 0, similar or slightly greater; 1, 1.5–2x; 2, more than 2x (Esposito, 2011; Esposito et al., 2017, 2018).
68. Metasoma length relative to length of prosoma and mesosoma (♀): 0, similar or slightly greater; 1, 1.5–2x; 2, more than 2x; ?, unknown (Lamoral, 1978; Prendini 2001, 2003; Esposito, 2011; Esposito et al., 2017, 2018).

Telson

69. Telson shape and length (♂): 0, spherical, length similar to width; 1, slightly ovate, length approximately 1.5x width; 2, ovate, length more than 2x width (Esposito, 2011; Esposito et al., 2017, 2018).
70. Telson vesicle, width in relation to width of metasomal segment V (♂): 0, similar; 1, narrower; 2, much narrower, less than half (Lamoral, 1978; Prendini 2001, 2003; Esposito, 2011; Esposito et al., 2017, 2018).
71. Telson vesicle, ventromedian carinae: 0, present; 1, absent (E.S. Volschenk and L. Prendini, unpublished data; Esposito, 2011; Esposito et al., 2017, 2018).
72. Telson vesicle, ventrolateral carinae: 0, present; 1, absent (E.S. Volschenk and L. Prendini, unpublished data; Esposito, 2011; Esposito et al., 2017, 2018).
73. Telson aculeus angle: 0, angled approximately 90° to vesicle; 1, angled less than 90° to vesicle (Esposito, 2011).
74. Telson vesicle, proximal margin, notch: 0, absent; 1, present, unmodified; 2, present, projecting vertically (Esposito, 2011).
75. Telson vesicle, lateral lobes: 0, absent; 1, present (Esposito, 2011).
76. Telson ventral surface: 0, granular; 1, smooth (Esposito, 2011).
77. Telson subaculear tubercle: 0, distinct, singular; 1, distinct, bifurcate; 2, obsolete, slight protuberance; 3, absent (Lamoral, 1980; Stockwell, 1989; Prendini, 2001, 2003; Esposito, 2011; Esposito et al., 2017, 2018).

Total length

78. Total length, sexual dimorphism: 0, male shorter than or similar to female; 1, male much longer than female; ?, unknown (Esposito, 2011; Esposito et al., 2017, 2018).

Ovariuterus

79. Number of loops ('cells'): 0, eight; 1, nine; ?, unknown (Volschenk et al., 2008; Esposito, 2011; Esposito et al., 2017, 2018).

80. Loop shape: 0, simple; 1, complex bridged; ?, unknown (Volschenk et al., 2008; Esposito, 2011; Esposito et al., 2017, 2018).

Book lungs

81. Lamellar surface: 0, slender venation; 1, ribbed venation; ?, unknown (Kamenz and Prendini, 2008; Esposito, 2011; Esposito et al., 2017, 2018).

82. Lamellar edge: 0, thorns; 1, smooth or wrinkled; ?, unknown (Kamenz and Prendini, 2008; Esposito, 2011; Esposito et al., 2017, 2018).

83. Spiracle, posterior margin: 0, hilocks; 1, subconical; ?, unknown (Kamenz and Prendini, 2008; Esposito, 2011; Esposito et al., 2017, 2018).

Color and infuscation

84. Cheliceral manus, reticulate infuscation: 0, present; 1, laterally restricted; 2, absent (Esposito, 2011).

85. Pedipalp segments, color pattern: 0, chela manus and patella similar to femur; 1, chela manus darker than femur; 2, chela manus and patella darker than femur; 3, chela manus paler than femur (Esposito, 2011).

86. Pedipalp femur, mottled infuscation: 0, present; 1, absent (Esposito, 2011).

87. Pedipalp patella, mottled infuscation: 0, present; 1, absent (Esposito, 2011).

88. Pedipalp chela manus, mottled infuscation: 0, present; 1, absent (Esposito, 2011).

89. Pedipalp chela fingers, mottled infuscation: 0, present; 1, absent (Esposito, 2011).

90. Tergites I–VI, mottled infuscation: 0, present; 1, absent (Esposito, 2011).

91. Tergites I–VI, lateral band of infuscation, shape: 0, absent; 1, narrow; 2, distinct, rectangular; 3, wide, almost touching lateral margins (Esposito, 2011).

92. Tergites I–VI, lateral band of infuscation, intensity: 0, absent; 1, faint; 2, mottled; 3, distinct (Esposito, 2011).

93. Tergites I–VI, infuscation: 0, eye-shaped pattern; 1, absent (Esposito, 2011).

94. Tergites I–VI, lateral margins infuscation: 0, distinct black line; 1, absent; ?, unknown (Esposito, 2011).

95. Tergites I–VI, median stripe of infuscation: 0, absent; 1, present (Esposito, 2011).

96. Tergite VII, color pattern: 0, similar to other tergites; 1, paler than other tergites (Esposito, 2011).

97. Carapace, mottled infuscation: 0, present; 1, absent (Esposito, 2011).

98. Carapace, bands of infuscation: 0, absent; 1, two broad bands; 2, four narrow lines (Esposito, 2011).

99. Carapace, interocular triangle infuscation: 0, present; 1, absent (Esposito, 2011).

100. Metasomal segments I–V, ventral surfaces, mottled infuscation: 0, present; 1, absent (Esposito, 2011).

101. Metasomal segments I–V, lateral surfaces, mottled infuscation: 0, present; 1, absent (Esposito, 2011).

102. Metasomal segments I–V, ventromedian stripe of infuscation: 0, present; 1, absent (Esposito, 2011).

103. Metasomal segment V, color pattern: 0, similar to preceding segments; 1, darker than preceding segments (Esposito, 2011; Esposito et al., 2017, 2018).

104. Telson, lateral bands of infuscation: 0, present; 1, absent (Esposito, 2011).

105. Telson, median stripe of infuscation: 0, complete; 1, posteriorly confined; 2, absent (Esposito, 2011).

106. Telson, mottled infuscation: 0, present; 1, absent (Esposito, 2011).

107. Sternites III–VI, mottled infuscation: 0, present; 1, absent (Esposito, 2011).

108. Sternite V, pale surface (♂): 0, present; 1, absent; ?, unknown (Esposito, 2011).
109. Sternite V, pale surface (♀): 0, present; 1, absent; ?, unknown (Esposito, 2011).
110. Sternite VII, color pattern: 0, similar to other sternites; 0, paler than preceding sternites; 2, darker than preceding sternites (Esposito, 2011).
111. Legs I–IV, dorsal surfaces, mottled infuscation: 0, present; 1, absent (Esposito, 2011).
112. Legs I–IV, ventral surfaces, mottled infuscation: 0, present; 1, absent (Esposito, 2011).

References

1. Wandeler, P.; Hoeck, P.E.; Keller, L.F. Back to the future: Museum specimens in population genetics. *Trends Ecol. Evol.* **2007**, *22*, 634–642. [CrossRef] [PubMed]
2. Zimmermann, J.; Hajibabaei, M.; Blackburn, D.C.; Hanken, J.; Cantin, E.; Posfai, J.; Evans, T.C. DNA damage in preserved specimens and tissue samples: A molecular assessment. *Front. Zool.* **2008**, *5*, 18. [CrossRef]
3. Dean, M.D.; Ballard, J.W. Factors affecting mitochondrial DNA quality from museum preserved *Drosophila simulans*. *Entomol. Exp. Appl.* **2001**, *98*, 279–283. [CrossRef]
4. Evans, T. DNA damage. *NEB Expr.* **2007**, *2*, 1–3.
5. Cárdenas, P.; Moore, J.A. First records of *Geodia* demosponges from the New England seamounts, an opportunity to test the use of DNA mini-barcodes on museum specimens. *Mar. Biodivers.* **2019**, *49*, 163–174. [CrossRef]
6. Francis, C.M.; Borisenko, A.V.; Ivanova, N.V.; Eger, J.L.; Lim, B.K.; Guillén-Servent, A.; Kruskop, S.V.; Mackie, I.; Hebert, P.D. The role of DNA barcodes in understanding and conservation of mammal diversity in Southeast Asia. *PLoS ONE* **2010**, *5*, e12575. [CrossRef] [PubMed]
7. Hebert, P.D.; Penton, E.H.; Burns, J.M.; Janzen, D.H.; Hallwachs, W. Ten species in one: DNA barcoding reveals cryptic species in the neotropical skipper butterfly *Astraptes fulgerator*. *Proc. Natl. Acad. Sci. USA* **2004**, *101*, 14812–14817. [CrossRef] [PubMed]
8. Meusnier, I.; Singer, G.A.; Landry, J.F.; Hickey, D.A.; Hebert, P.D.; Hajibabaei, M. A universal DNA mini-barcode for biodiversity analysis. *BMC Genom.* **2008**, *9*, 214. [CrossRef]
9. Alberdi, A.; Garin, I.; Aizpurua, O.; Aihartza, J. The foraging ecology of the mountain long-eared bat *Plecotus macrobullaris* revealed with DNA mini-barcodes. *PLoS ONE* **2012**, *7*, e35692. [CrossRef]
10. Bagley, J.C.; De Aquino, P.D.; Breitman, M.F.; Langeani, F.; Colli, G.R. DNA barcode and minibarcode identification of freshwater fishes from Cerrado headwater streams in central Brazil. *J. Fish Biol.* **2019**, *95*, 1046–1060. [CrossRef]
11. Dong, W.; Liu, H.; Xu, C.; Zuo, Y.; Chen, Z.; Zhou, S. A chloroplast genomic strategy for designing taxon specific DNA mini-barcodes: A case study on ginsengs. *BMC Genet.* **2014**, *15*, 138. [CrossRef]
12. Dubey, B.; Meganathan, P.R.; Haque, I. DNA mini-barcoding: An approach for forensic identification of some endangered Indian snake species. *Forensic Sci. Int. Genet.* **2011**, *5*, 181–184. [CrossRef] [PubMed]
13. Sultana, S.; Ali, M.E.; Hossain, M.M.; Naquiah, N.; Zaidul, I.S. Universal mini COI barcode for the identification of fish species in processed products. *Food Res. Int.* **2018**, *105*, 19–28. [CrossRef]
14. Wannell, G.J.; Griffiths, A.M.; Spinou, A.; Batista, R.; Mendonça, M.B.; Wosiacki, W.B.; Fraser, B.; Wintner, S.; Papadopoulos, A.I.; Krey, G.; et al. A new minibarcode assay to facilitate species identification from processed, degraded or historic ray (Batoidea) samples. *Conserv. Genet. Resour.* **2020**, *18*, 659–668. [CrossRef]
15. Yang, F.; Ding, F.; Chen, H.; He, M.; Zhu, S.; Ma, X.; Jiang, L.; Li, H. DNA barcoding for the identification and authentication of animal species in traditional medicine. *Evid.-Based Complement. Altern. Med.* **2018**, *2018*, 5160254. [CrossRef] [PubMed]
16. de Armas, L.F. Presencia de *Centruroides schmidti* Sissom en el sureste de Mexico y descripcion de dos especies nuevas (Scorpiones: Buthidae). *Rev. Nicar. Entomol.* **1996**, *36*, 21–33.
17. Hoffmann, C.C. Monografias para la entomología médica de México. Monografia No. 2, Los escorpiones de México. Segunda parte: Buthidae. *An. Inst. Biol. Univ. Nac. Autón. México* **1932**, *3*, 243–361.
18. Martín-Frías, E.; de Armas, L.F.; Paniagua-Solís, J.F. Redescription of the Mexican scorpion *Centruroides hoffmanni* Armas, 1996 (Scorpiones: Buthidae). *Euscorpius* **2005**, *2005*, 1–7. [CrossRef]
19. Sissom, W.D. Redescription of the scorpion *Centruroides thorelli* Kraepelin (Buthidae) and description of two new species. *J. Arachnol.* **1995**, *23*, 91–99.
20. Ponce-Saavedra, J.; Moreno-Barajas, R.J. El género *Centruroides* Marx 1890 (Scorpiones: Buthidae) en México. *Biológicas* **2005**, *7*, 42–51.
21. Esposito, L.A.; Prendini, L. Island ancestors and New World biogeography: A case study from the scorpions (Buthidae: Centruroidinae). *Sci. Rep.* **2019**, *9*, 3500. [CrossRef]
22. Esposito, L. Systematics and Biogeography of the New World Scorpion Genus *Centruroides* Marx, 1890 (Scorpiones: Buthidae). Ph.D. Dissertation, City University of New York, New York, NY, USA, 2011.
23. Goodman, A.; Prendini, L.; Francke, O.F.; Esposito, L.A. Systematic revision of the arboreal Neotropical "*thorellii*" clade of *Centruroides* Marx, 1890, bark scorpions (Buthidae C.L. Koch, 1837) with descriptions of six new species. *Bull. Am. Mus. Nat. Hist.* **2021**, *452*, 1–92.

24. Folmer, R.H.; Nilges, M.; Folkers, P.J.; Konings, R.N.; Hilbers, C.W. A model of the complex between single-stranded DNA and the single-stranded DNA binding protein encoded by gene V of filamentous bacteriophage M13. *J. Mol. Biol.* **1994**, *240*, 341–357. [CrossRef] [PubMed]
25. Arango, C.P.; Wheeler, W.C. Phylogeny of the sea spiders (Arthropoda, Pycnogonida) based on direct optimization of six loci and morphology. *Cladistics* **2007**, *23*, 255–293. [CrossRef]
26. Kearse, M.; Moir, R.; Wilson, A.; Stones-Havas, S.; Cheung, M.; Sturrock, S.; Thierer, T. Geneious Basic: An integrated and extendable desktop software platform for the organization and analysis of sequence data. *J. Bioinform.* **2012**, *28*, 1647–1649. [CrossRef]
27. Esposito, L.A.; Yamaguti, H.Y.; Pinto-da-Rocha, R.; Prendini, L. Plucking with the plectrum: Phylogeny of the New World buthid scorpion subfamily Centruroidinae Kraus, 1955 (Scorpiones: Buthidae) reveals evolution of three pecten-sternite stridulation organs. *Arthropod Syst. Phylogeny* **2018**, *76*, 87–122.
28. Hjelle, J.T. Anatomy and morphology. In *The Biology of Scorpions*; Polis, G.A., Ed.; Stanford University Press: Stanford, CA, USA, 1990; pp. 9–63.
29. Sissom, W.D. Systematics, biogeography and paleontology. In *The Biology of Scorpions*; Polis, G.A., Ed.; Stanford University Press: Stanford, CA, USA, 1990; pp. 64–160.
30. Vachon, M. *Études sur les Scorpions*; Institut Pasteur d'Algérie: Algiers, Algeria, 1952; 482p.
31. Vachon, M. Étude des caractères utilisés pour classer les familles et les genres de scorpions (Arachnides). 1. La trichobothriotaxie en arachnologie. Sigles trichobothriaux et types de trichobothriotaxie chez les scorpions. *Bull. Mus. Hist. Nat. Paris* **1974**, *140*, 857–958.
32. Prendini, L. Phylogeny and classification of the superfamily Scorpionoidea Latreille 1802 (Chelicerata, Scorpiones): An exemplar approach. *Cladistics* **2000**, *16*, 1–78. [CrossRef]
33. Kamenz, C.; Prendini, L. An atlas of book lung fine structure in the order Scorpiones (Arachnida). *Bull. Am. Mus. Nat. Hist.* **2008**, *316*, 1–359. [CrossRef]
34. Volschenk, E.S.; Mattoni, C.I.; Prendini, L. Comparative anatomy of the mesosomal organs of scorpions (Chelicerata, Scorpiones), with implications for the phylogeny of the order. *Zool. J. Linn. Soc.* **2008**, *154*, 651–675. [CrossRef]
35. Larkin, M.A.; Blackshields, G.; Brown, N.P.; Chenna, R.; McGettigan, P.A.; McWilliam, H.; Thompson, J.D. Clustal W and Clustal X version 2.0. *J. Bioinform.* **2007**, *23*, 2947–2948. [CrossRef]
36. Thompson, J.D.; Higgins, D.G.; Gibson, T.J. CLUSTAL W: Improving the sensitivity of progressive multiple sequence alignment through sequence weighting, position-specific gap penalties and weight matrix choice. *Nucleic Acids. Res.* **1994**, *22*, 4673–4680. [CrossRef] [PubMed]
37. Maddison, W.P.; Maddison, D.D. Mesquite: A Modular System for Evolutionary Analysis. Version 3.4. Available online: https://www.mesquiteproject.org (accessed on 20 June 2020).
38. Ronquist, F.; Huelsenbeck, J.P. MrBayes, 3, Bayesian phylogenetic inference under mixed models. *J. Bioinform.* **2003**, *19*, 1572–1574. [CrossRef]
39. Stamatakis, A. RAxML version, 8, A tool for phylogenetic analysis and post-analysis of large phylogenies. *J. Bioinform.* **2014**, *30*, 1312–1313. [CrossRef]
40. Miller, M.A.; Pfeiffer, W.; Schwartz, T. Creating the CIPRES Science Gateway for inference of large phylogenetic trees. In Proceedings of the Gateway Computing Environments Workshop (GCE), New Orleans, LA, USA, 14 November 2010; pp. 1–8.
41. Lanfear, R.; Frandsen, P.B.; Wright, A.M.; Senfeld, T.; Calcott, B. PartitionFinder, 2: New methods for selecting partitioned models of evolution for molecular and morphological phylogenetic analyses. *Mol. Biol. Evol.* **2017**, *34*, 772–773. [CrossRef] [PubMed]
42. Lewis, P.O. A likelihood approach to estimating phylogeny from discrete morphological character data. *Syst. Biol.* **2001**, *50*, 913–925. [CrossRef] [PubMed]
43. Alfaro, M.E.; Zoller, S.; Lutzoni, F. Bayes or bootstrap? A simulation study comparing the performance of Bayesian Markov Chain Monte Carlo sampling and bootstrapping in assessing phylogenetic confidence. *Mol. Biol. Evol.* **2003**, *20*, 255–266. [CrossRef]
44. Masters, B.C.; Fan, V.; Ross, H.A. Species delimitation—A Geneious plugin for the exploration of species boundaries. *Mol. Ecol. Resour.* **2011**, *11*, 154–157. [CrossRef]
45. Rosenberg, N.A. Statistical tests for taxonomic distinctiveness from observations of monophyly. *J. Evol.* **2007**, *61*, 317–323. [CrossRef]
46. Moritz, C.; Cicero, C.; Godfray, C. DNA barcoding: Promise and pit-falls. *PLoS Biol.* **2004**, *2*, e354. [CrossRef]
47. Yeo, D.; Srivathsan, A.; Meier, R. Longer is not always better: Optimizing barcode length for large-scale species discovery and identification. *Syst Biol.* **2020**, *69*, 999–1015. [CrossRef] [PubMed]
48. Larena, I.; Salazar, O.; Gonzalez, V.; Julian, M.C.; Rubio, V. Design of a primer for ribosomal DNA internal transcribed spacer with enhanced specificity for ascomycetes. *J. Biotechnol.* **1999**, *75*, 187–194. [CrossRef]
49. Colgan, D.J.; McLauchlan, A.; Wilson, G.D.F.; Livingston, S.P.; Edgecombe, G.D.; Macaranas, J.; Cassis, G.; Gray, M.R. Histone H3 and U2 snRNA DNA sequences and arthropod molecular evolution. *Aust. J. Zool.* **1998**, *46*, 419–437. [CrossRef]
50. Johnson, N.K.; Cicero, C. New mitochondrial DNA data affirm the importance of Pleistocene speciation in North American birds. *Evolution* **2004**, *58*, 1122–1130. [CrossRef]
51. Rodrigo, A.; Bertels, F.; Heled, J.; Noder, R.; Shearman, H.; Tsai, P. The perils of plenty: What are we going to do with all these genes? *Philos. Trans. R. Soc. B* **2008**, *363*, 3893–3902. [CrossRef]

52. Goodman, A.; Esposito, L. Niche partitioning in congeneric scorpions. *Invertebr. Biol.* **2020**, *139*, e12280. [CrossRef]
53. Johnson, J.D.; Mata-Silva, V.; García-Padilla, E.; Wilson, L.D. The herpetofauna of Chiapas, Mexico: Composition, physiographic distribution, and conservation status. *Mesoam. Herpetol.* **2015**, *2*, 272–329.
54. Towler, W.I. Phylogenetic Structure of Two Central Mexican *Centruroides* Species Complexes. Master's Thesis, Marshall University, Huntington, WV, USA, 2002.
55. Ponce Saavedra, J.; Francke, O.F. Una nueva especie de alacrán del género *Centruroides* Marx 1890 (Scorpiones, Buthidae) de la depresión del Balsas, México. *Acta Zool. Mex.* **2004**, *20*, 221–232.
56. Saavedra, J.P.; Sissom, W.D. A new species of the genus *Vaejovis* (Scorpiones, Vaejovidae) endemic to the Balsas basin of Michoacán, Mexico. *J. Arachnol.* **2004**, *32*, 539–544. [CrossRef]
57. Mendoza, J.; Francke, O.F. Systematic revision of *Brachypelma* red-kneed tarantulas (Araneae: Theraphosidae), and the use of DNA barcodes to assist in the identification and conservation of CITES-listed species. *Invert. Syst.* **2017**, *31*, 157–179. [CrossRef]
58. Meyer, S.E.; García-Moya, E.; Lagunes-Espinoza, L.D.C. Topographic and soil surface effects on gypsophile plant community patterns in central Mexico. *J. Veg. Sci.* **1992**, *3*, 429–438. [CrossRef]
59. Ødegaard, F. How many species of arthropods? Erwin's estimate revised. *Biol. J. Linn. Soc.* **2000**, *71*, 583–597. [CrossRef]